Available online at www.sciencedirect.com
SCIENCE DIRECT®
International Journal of Heat and Mass Transfer 47 (2004) 1761–1769
International Journal of HEAT and MASS TRANSFER
www.elsevier.com/locate/ijhmt

Mixed convection in two-sided lid-driven differentially heated square cavity

Hakan F. Oztop [a,*,1], Ihsan Dagtekin [b]

[a] Ecole Polytechnique, Genie Mecanique, C.P. 6079, Montreal, Que., Canada H3C 3A7
[b] Department of Mechanical Engineering, Fırat University, Elazig, Turkey

Received 6 December 2002; received in revised form 15 October 2003

Abstract

Steady state two-dimensional mixed convection problem in a vertical two-sided lid-driven differentially heated square cavity is investigated numerically. The left and right moving walls are maintained at different constant temperatures while upper and bottom walls are thermally insulated. Three cases were considered depending on the direction of moving walls. Richardson number, $Ri = Gr/Re^2$ emerges as a measure of relative importance of natural and forced convection modes on the heat transfer. Governing parameters were $0.01 < Ri < 100$ and $Pr = 0.7$. It is found that both Richardson number and direction of moving walls affect the fluid flow and heat transfer in the cavity. For $Ri < 1$ the influence of moving walls on the heat transfer is the same when they move in opposite direction regardless of which side moves upwards and it is reduced when both move upwards. For the case of opposing buoyancy and shear forces and for $Ri > 1$, the heat transfer is somewhat better due to formation of secondary cells on the walls and a counter rotating cell at the center.

1. Introduction

Mixed convection problem with lid-driven flows in enclosures are encountered in a variety of engineering applications including cooling of electronic devices, furnaces, lubrication technologies, chemical processing equipment, drying technologies, etc.

Fluid flow and heat transfer in rectangular or square cavities driven by buoyancy and shear have been studied extensively in the literature. A review shows that there are two kinds of studies: the first one is concerned with horizontal top [1–10] or bottom [11] wall sliding lid-driven two-dimensional cavities, in which the top wall has a constant velocity [1–3] or oscillating [4,5], and similarly in three dimensional cavities [6,7,9,10,16]. Other solid walls in these cases are at various boundary conditions. The second deals with side driven differentially heated cavities. In this case, left or right vertical wall or both vertical walls move with a constant velocity in their planes [12,13]. In these studies usually the lid-driven side and the one opposing it are heated differentially to create a temperature gradient in the cavity. Combination of buoyancy forces due to temperature gradient and forced convection due to shear results in a mixed convection heat transfer, which is a complex phenomenon due to interaction of these forces. Our concern in this study is being of the second kind, we will briefly review the literature on side driven differentially heated cavities.

Arpaci and Larsen [12] have presented an analytical treatment of the mixed convection heat transfer in tall cavities, which had one vertical side moving, vertical boundaries at different temperatures and horizontal boundaries adiabatic. They showed that in this particular case, the forced and buoyancy-driven parts of the problem could be solved separately and combined to obtain the general mixed convection problem. Aydın

* Corresponding author. Tel.: +90-424-2370-000; fax: +90-424-2415-526.
E-mail address: hakan.oztop@polymtl.ca (H.F. Oztop).
[1] On leave from Department of Mechanical Engineering, Fırat University, Elazig, Turkey.

0017-9310/$ - see front matter © 2003 Elsevier Ltd. All rights reserved.
doi:10.1016/j.ijheatmasstransfer.2003.10.016

Nomenclature

A	aspect ratio, H/L
g	gravitational acceleration, m/s^2
Gr	Grashof number, $g\beta H^3\Delta T/v^2$
H	cavity height, m
L	cavity width, m
Nu	Nusselt number, hH/k
P	pressure, Pa
Pr	Prandtl number, v/α
Re	Reynolds number, V_pL/v
Ri	Richardson number, Gr/Re^2
T	temperature, K
u, v	dimensionless velocities in x- and y-direction
V_p	lid-driven plate velocity, m/s
x', y'	cartesian coordinates
x, y	dimensionless cartesian coordinates, x'/L, y'/L

Greek symbols

v	kinematic viscosity, m^2/s
α	thermal diffusivity, m^2/s
ρ	density, kg/m^3
μ	dynamic viscosity, kg/m s
ψ	stream function
β	thermal expansion coefficient, 1/K
θ	dimensionless temperature
φ	depended variable

Superscript

k	iteration number

Subscripts

c	cold wall
h	hot wall
p	plate
w	wall

[13] studied numerically mechanisms of aiding and opposing forces in a shear and buoyancy-driven cavity. The square cavity had one vertical hot wall moving upwards or downwards, the opposite cold wall fixed, and both horizontal walls adiabatic. He carried out a parametric study for Gr/Re^2 from 0.01 to 100 with $Pr = 0.71$ fluids and identified three kinds of heat transfer regime: forced convection dominated, mixed and buoyancy dominated regime. He determined further that mixed convection range of Gr/Re^2 for opposing-buoyancy case was wider than that of the aiding-buoyancy case, although he did not present any quantitative information regarding these regimes and heat transfer characteristics.

Kuhlmann et al. [14] conducted a numerical and experimental study on steady flow in rectangular two-sided lid-driven cavities. They found that the basic two-dimensional flow was not always unique. For low Reynolds numbers it consist two separate co-rotating vortices adjacent to the moving walls. Blohm and Kuhlmann [15] studied experimentally incompressible fluid flow in a rectangular container driven by two facing side walls which move steadily in anti-parallel for Reynolds numbers up to 1200. The moving sidewalls are realized by two rotating cylinders of large radii tightly closing the cavity. They found that beyond a first threshold robust, steady, three-dimensional cells bifurcate supercritically out of the basic flow state. If both side walls move with same velocity (symmetrical driving) the oscillatory instability was found to be tricritical.

Indirectly related to the present study, two-sided lid-driven shallow cavities were studied by Alleborn et al. [16]. They studied heat and mass transfer in a two-sided shallow cavity having an aspect ratio of 5, which had both moving bottom hot wall and top cool wall, and two others adiabatic. They determined the effect of Reynolds number and concentration in cavities at different angles, i.e., with horizontal and vertical orientation of the cavity, by using vorticity-stream function approach. They found that cavity length and velocity were parameters affecting the mass transfer and established two turning points and flow configurations in which heat and mass transfer were minimized.

The previous studies clearly show that lid-driven differentially heated cavities have interesting applications in various fields and the mixed convection with two-sided lid-driven differentially heated cavities has not been addressed. Depending on the applications, various interactions between natural and forced convection should be known, the governing parameters and their effects on heat transfer should be established. The aim of this study is to investigate this case in differentially heated square cavities in which both vertical sides are moving and both horizontal sides are adiabatic.

2. Problem description

The definition sketch of the problem and the boundary conditions are shown in Fig. 1. It is a two-sided lid-driven square cavity filled with an incompressible fluid. The vertical lids have different constant temperatures. The horizontal walls are adiabatic. Three different cases were considered as shown in Fig. 1. In case I, the left wall (cold) is moving up while right wall (hot) is moving down. In case II, the left wall is moving down while the right upwards, and in case III both walls are moving upwards. In all three cases the moving walls

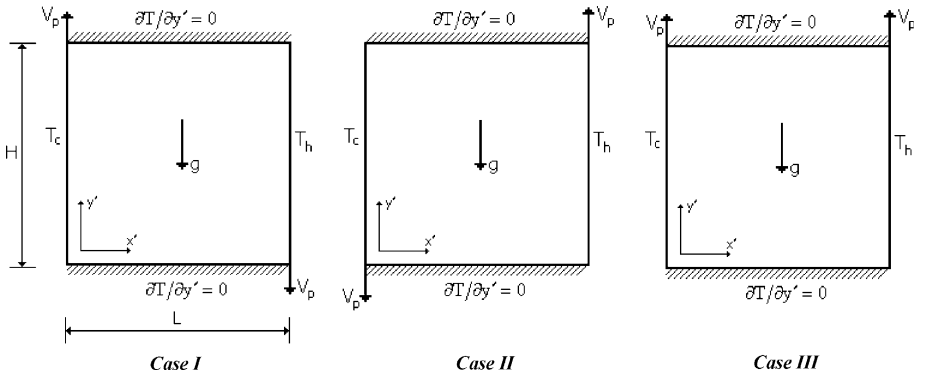

Fig. 1. Physical model for three cases and the coordinate system.

have the same speed and gravitational force direction is parallel to the moving walls.

3. Mathematical modeling

It is assumed that the flow is two-dimensional, steady state, laminar and the fluid is incompressible. In fact, experimental results with lid-driven cavities [14] have shown that two-dimensional solution is acceptable for small *Re* numbers, which is the case in this study. The thermophysical properties of the fluid at a reference temperature are assumed to be constant, except in the buoyancy term of the momentum equation, i.e., the Boussinesq approximation. It is further assumed that radiation heat transfer among sides is negligible with respect to other modes of heat transfer. In the light of assumptions mentioned above, the non-dimensional continuity, momentum and energy equations can be written as follows:

$$\frac{\partial u}{\partial x}+\frac{\partial v}{\partial y}=0 \tag{1}$$

$$u\frac{\partial u}{\partial x}+v\frac{\partial u}{\partial y}=-\frac{\partial P}{\partial x}+\frac{1}{Re}\left(\frac{\partial^2 u}{\partial x^2}+\frac{\partial^2 u}{\partial y^2}\right) \tag{2}$$

$$u\frac{\partial v}{\partial x}+v\frac{\partial v}{\partial y}=-\frac{\partial P}{\partial y}+\frac{1}{Re}\left(\frac{\partial^2 v}{\partial x^2}+\frac{\partial^2 v}{\partial y^2}\right)+\frac{Gr}{Re^2}\theta \tag{3}$$

$$u\frac{\partial \theta}{\partial x}+v\frac{\partial \theta}{\partial y}=\frac{1}{RePr}\left(\frac{\partial^2 \theta}{\partial x^2}+\frac{\partial^2 \theta}{\partial y^2}\right) \tag{4}$$

The following non-dimensional variables are defined

$$\left.\begin{aligned} &x=\frac{x'}{L},\quad y=\frac{y'}{L},\quad u=\frac{u'}{V_p},\quad v=\frac{v'}{V_p},\quad p=\frac{p'}{\rho V_p^2}\\ &\theta=\frac{T-T_c}{T_h-T_c},\quad Gr=\frac{g\beta H^3\Delta\theta}{\nu^2},\quad Re=\frac{V_p L}{\nu},\quad Pr=\frac{\nu}{\alpha}\end{aligned}\right\} \tag{5}$$

Boundary conditions are isothermal on the vertical moving lids and adiabatic on the horizontal walls. On the horizontal walls, u and v velocities are zero and lids have a constant velocity. The relevant boundary conditions are given as follows:

$$\left.\begin{aligned} &x=0,\ 0<y<1,\ u=0,\ v=1 \text{ or } (v=-1),\ \theta=\theta_c\\ &x=1,\ 0<y<1,\ u=0,\ v=1 \text{ or } (v=-1),\ \theta=\theta_h\\ &y=0,\ 0<x<1,\ u=v=0,\ \partial\theta/\partial y=0\\ &y=1,\ 0<x<1,\ u=v=0,\ \partial\theta/\partial y=0\end{aligned}\right\} \tag{6}$$

Local Nusselt number is

$$Nu_y=-\frac{1}{A}(\partial\theta/\partial x)_w/(\theta_h-\theta_c) \tag{7}$$

The average Nusselt number is calculated by integrating the local Nusselt number along the wall

$$\overline{Nu}=\frac{1}{A}\int_0^1 Nu_y\,dx \tag{8}$$

The stream function is calculated from its definition

$$u=\frac{\partial\psi}{\partial y},\quad v=-\frac{\partial\psi}{\partial x} \tag{9}$$

It is taken $\psi=0$ at the solid boundaries.

4. Numerical solution of governing equations

The discretization procedure of the governing equations is based on a finite control volume using the non-staggered grid arrangement with the SIMPLEM algorithm [17]. The mathematical details of the discretization process can be found in the literature [18].

The validation of present computer code has been verified for the mixed convection in a lid-driven cavity with a stable vertical temperature gradient problem by Iwatsu et al. [2]. As can be seen from Table 1 there is a

Table 1
The comparison of average Nusselt number values with Iwatsu et al. [2]

Ri number	Iwatsu et al. [2] $\overline{Nu}$	This study $\overline{Nu}$
1.00	1.34	1.33
0.06	3.62	3.60
0.01	6.29	6.21

good agreement for average Nusselt numbers obtained in the present study when compared to those of [2].

Numerical experiments were performed in order to check the grid independence of the solutions. Three different grid sizes (81×81, 61×61 and 41×41) were used and (61×61) grid points were adopted for grid-free solution throughout the calculations in the present study. This grid dimension has shown a negligible deviation in Nusselt number (0.17%). To obtain finite difference equations, power law difference scheme (PLDS) for convective terms, central difference scheme (CDS) for diffusion terms were used [18]. The absolute convergence criterion of ($|\phi^k - \phi^{k-1}| < 10^{-4}$) was used for the termination of all computations, where φ $(u, v, T \ldots)$ is the depended variable in the partial differential equations and k is the iteration number. An under-relaxation parameter of 0.5 was used in order to obtain a stable convergence for the solution of momentum and energy equations while there was no need for such a parameter in the solution of pressure equation. Streamlines were generated from the axial velocity components as being $\psi = \int u\,\mathrm{d}y$ integration over physical domain. In a typical computation, about 2000 iterations were required to obtain the convergence.

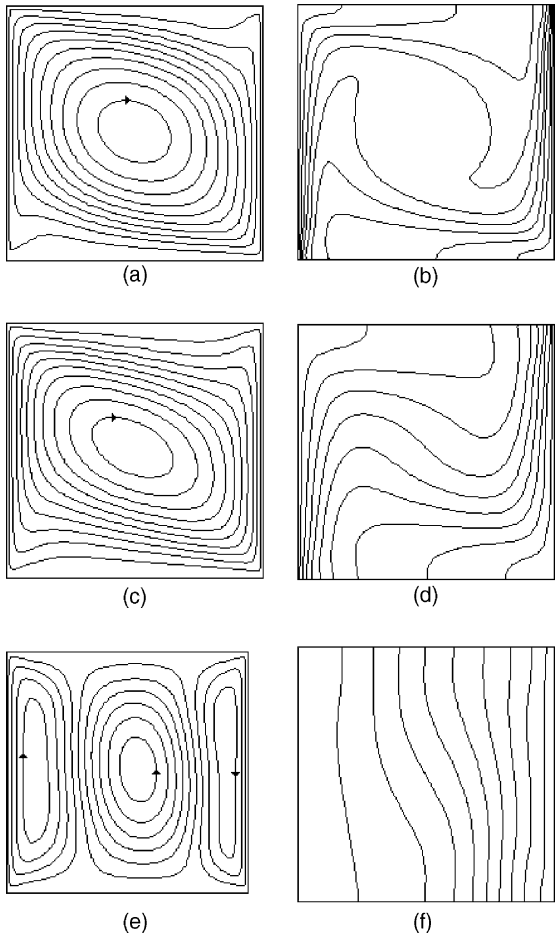

Fig. 2. Streamlines (on the left) and isotherms (on the right) for case I: (a–b) $Ri = 0.1$, (c–d) $Ri = 1$, (e–f) $Ri = 10$.

5. Results and discussion

Mixed convection flow and temperature fields in two-sided lid-driven square cavity are examined. The governing parameters in this problem is Richardson number, $Ri = Gr/Re^2$, which characterizes the relative importance of buoyancy to forced convection. To vary Richardson number, Grashof number is fixed at $Gr = 10^4$ while changing Reynolds number through the plate velocity V_p. The calculations are done with Reynolds number identical at both sides of the cavity. Investigations through the cavity are made for ranges of the Richardson number from 0.01 to 100. Two-sided lid-driven cavity is analyzed according to the direction of moving plate in three cases shown in Fig. 1. The results for each will be presented next.

Case I: The left walls adjacent to left moving lid is moving upwards while the right wall moves downwards. It is noted that forces due to moving lids and buoyancy act in opposite directions. Streamlines (on the left) and isotherms (on the right) for $Ri = 0.1$–10 are shown in Fig. 2. For $Ri = 0.1$, Fig. 2a and b shows that the forced convection plays a dominant role and the recirculation flow is mostly generated only by moving lids. As it is seen from Fig. 2a the recirculation is clockwise and some perturbations are seen in streamlines in the upper right and lower left corners due to impingement of fluid to the horizontal wall. Even if the observed perturbations at the upper right and lower left corners are ignored, we can see that they are too different from streamlines and isotherms observed in a differentially heated cavity.

For these two cases of Fig. 2a and c, $|\psi_{ext}| = 6.98\times10^{-4}$, $x = 0.49$, $y = 0.51$ and $|\psi_{ext}| = 2.01\times10^{-4}$, $x = 0.54$, $y = 0.51$ respectively. For $Ri = 10$ in Fig. 2c and d, we observe, in addition to a main cell, appearance of two secondary cells: the main cell is formed at the center of the cavity, but the cell center not quite on the symmetry lines ($|\psi_{ext}| = 1.025\times10^{-5}$, $x = 0.58$ $y = 0.55$), while two other weaker cells are formed near the moving

walls. This is because the fluid rises along the right hot wall and sinks on the left cold wall due to forces generated by buoyancy and by shear. As a result two clockwise rotating cells are formed at each side and a clockwise rotating cell at the center makes the heat transfer from right to left possible. Similar phenomena have not been observed with one vertical sided lid-driven cavity in the literature, although at low Richardson numbers Aydın [13] has reported two cell formations. Isotherms in Fig. 2b, d and f show that as Richardson number increases the horizontal thermal gradient near the vertical walls decreases, as a result of which heat transfer decreases. This will be discussed next.

The details of velocity profiles at the vertical centerline and local Nusselt number along the cold wall are presented in Figs. 3 and 4 respectively. In Fig. 3, as Ri is increased to 10 the velocity profile turns to negative profile unlike for lower Richardson number. It is observed that, u velocity profiles become flatter with increasing of Richardson number, an indication of a stratified flow in the cavity, which is similar to ones obtained in case of natural convection in differentially heated cavities at high Grashof numbers, but values at $Ri > 10$ negative velocity profile formed on the upper part of the enclosure. For low Richardson numbers, the forced convection becomes dominant and a strong circulation is observed in the cavity.

Fig. 4 shows that following the observations made for Fig. 2, at low Richardson numbers, the local Nusselt number increases along the cold moving wall, hence, the heat removal is enhanced. At high Richardson numbers, the variation of Nusselt number is negligibly small, which is an expected outcome for natural convection dominated regime. But for lower Richardson number as

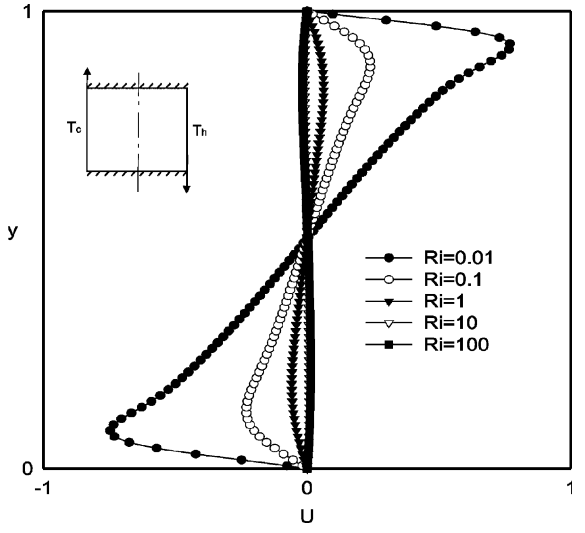

Fig. 3. Velocity profiles at the vertical centerline for case I.

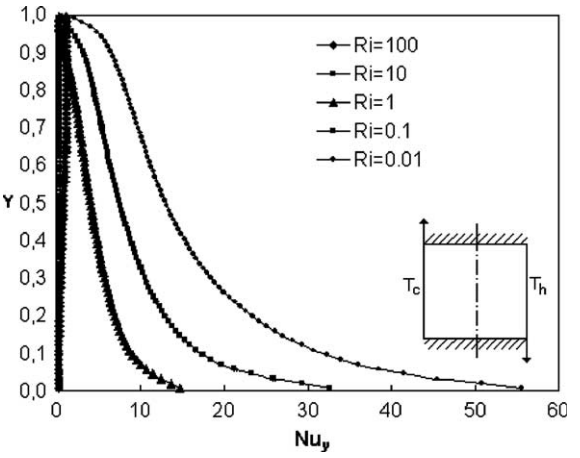

Fig. 4. Local Nusselt number along the cold wall for case I.

a result of different velocity profile (negative profile on the upper) local Nusselt number has been increased to some degree near the upper wall as seen in Fig. 4.

Case II: In this case, the left wall is moving downwards while the right wall upwards, which represents the case with aiding shear and buoyancy forces. Fig. 5 illustrates streamlines (on the left) and isotherms (on the right) for $Ri = 0.1$–10. The streamlines and isotherms for $Ri = 0.1$ and 1.0 in Fig. 5a and c respectively show a mirror image of those in Fig. 2a and c with circulation direction changing from clockwise to counter-clockwise due to moving plate directions. However, in order to check the validation of present study from point of view of flow field, streamline patterns given in Fig. 5a and c cold be compared with experimental study of Blohm and Khulmann [15]. It could be seen that there was qualitatively a good agreement between present study and experimental study of Ref. [15].

For this case, $|\psi_{\text{ext}}| = 7.187 \times 10^{-4}$, $x = 0.49$, $y = 0.51$, which shows the cell center has shifted only slightly to the left of the symmetry line, but the strength is relatively high due to forced convection. Isotherms show that the flow in the center of cavity is not much affected by the horizontal thermal gradient. They are restricted to the vertical cavity walls where thermal gradients are steeper, as a result of which, the heat transfer significantly increases.

Fig. 5c and d shows streamlines and isotherms for $Ri = 1$, in which case forced and natural convections are comparable. There is less significant effect of the moving lids on the streamlines and isotherms for this case. The isotherms are somewhat similar to those observed in differentially heated cavities but the streamlines are quite different. $|\psi_{\text{ext}}| = 2.08 \times 10^{-4}$, $x = 0.45$, $y = 0.51$, which shows the cell center shifted strongly to the left and its strength became lower.

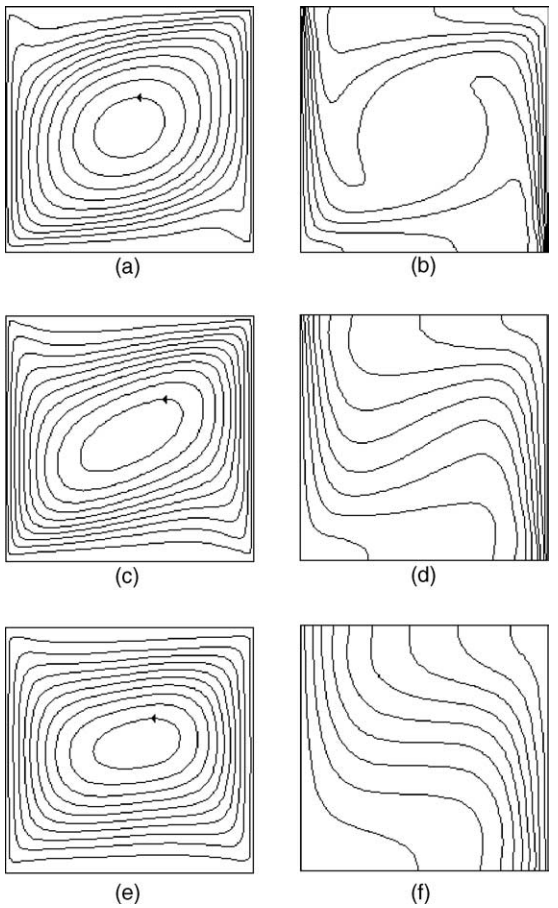

Fig. 5. Streamlines (on the left) and isotherms (on the right) for case II: (a–b) $Ri = 0.1$, (c–d) $Ri = 1$, (e–f) $Ri = 10$.

Fig. 5e and f shows the results for $Ri = 10$, in which case the buoyancy effect can be observed clearly. Since both vertical sides have the same Reynolds number and both moving in the opposite direction to that of buoyancy forces, excluding the perturbations at the corners the streamlines and isotherms in the cavity are quite similar to those usually obtained in a differentially heated cavity by natural convection. In this case, $|\psi_{ext}| = 3.94 \times 10^{-5}$, $x = 0.58$, $y = 0.51$. We can see that the strength of the circulation is reduced considerably and the center of the cell moved towards right. These observations reported here are not similar to those observed in one vertical sided lid-driven cavities [13].

To examine the flow and heat transfer in the cavity, velocity profiles at vertical centerline and local Nusselt number at the cold wall are produced and presented in Figs. 6 and 7 respectively. Fig. 6 shows velocity profiles for Richardson number from 0.01 to 100, which are almost symmetric in the lower and upper half of the cavity. As expected, it is seen that as Richardson number increases, u velocity profiles become flatter with velocities near zero along the vertical centerline. For small Richardson numbers, u velocity makes a peak near the left upper and lower elevations corresponding to the leading edge of moving wall.

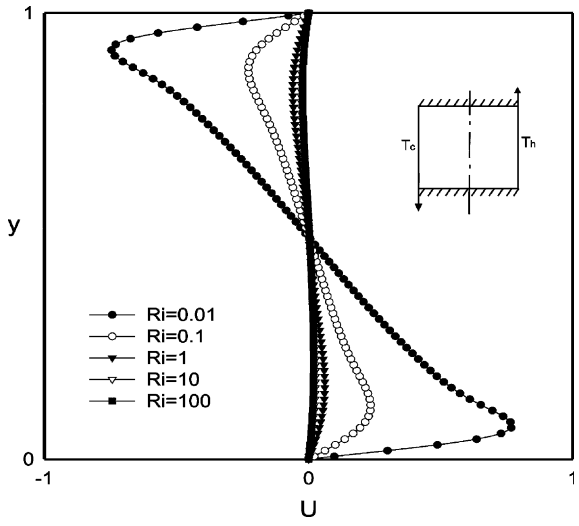

Fig. 6. Velocity profiles at the vertical centerline for case II.

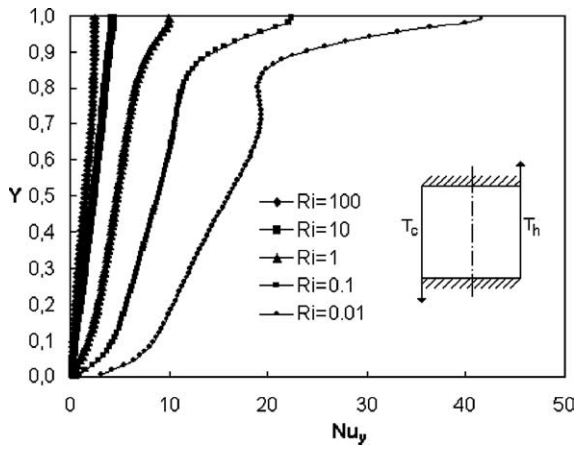

Fig. 7. Local Nusselt number along the cold wall for case II.

Fig. 7 shows that as Richardson number increases, the local Nusselt number decreases. This is expected since for increasing Richardson number, natural convection becomes dominant and the flow motion is generally subdued. As a result the heat transfer in the interior is dominated by conduction mode.

Case III: This is the case both vertical walls move upward in which aiding forces of buoyancy and shear are on the right and opposing forces are on the left. Therefore we should expect that main circulation will be on the right of the cavity. Streamlines and isotherms for Richardson number from 0.1 to 10 are presented in

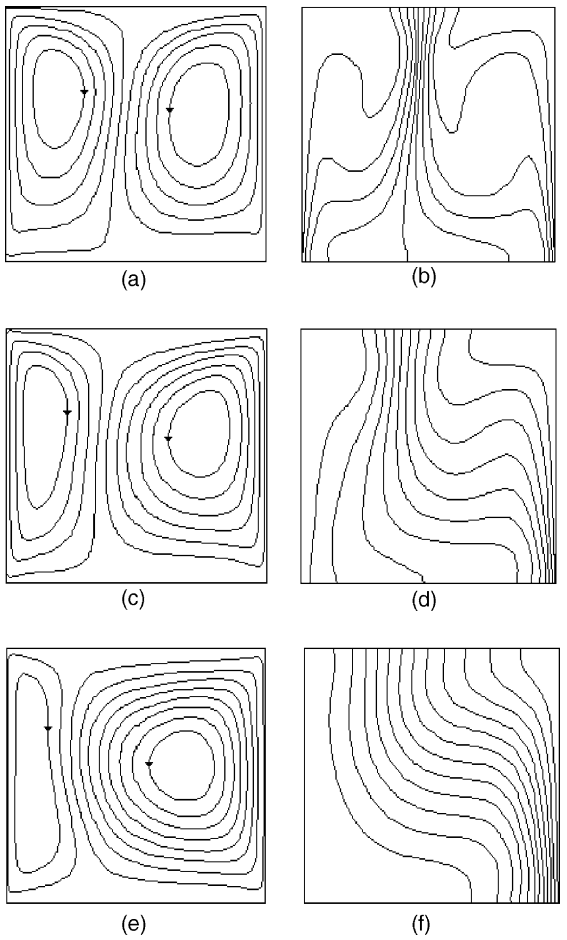

Fig. 8. Streamlines (on the left) and isotherms (on the right) for case III: (a–b) $Ri = 0.1$, (c–d) $Ri = 1$, (e–f) $Ri = 10$.

Fig. 8. Streamlines for $Ri = 0.1$ in Fig. 8a show two circulating cells, a counter-clockwise circulating cell on the right and clockwise circulating one on the left. For $Ri = 0.1$, for which the forced convection is dominant, the quasi-symmetrical behavior is an expected result due to relatively negligible buoyancy forces. However, as has been pointed out earlier, the one on the right is dominant due to aiding buoyancy and shear forces with $|\psi_{ext}| = 4.88 \times 10^{-4}$, $x = 0.74$, $y = 0.53$. Fig. 8b shows that the isotherms form quasi-symmetrical and steeper thermal gradients between two counter-circulating cells and no temperature gradient penetration is discernable around them. For $Ri = 1.0$ in Fig. 8c and d, i.e., buoyancy and shear forces are equally important, the aiding buoyancy driven force on the right affects the flow and temperature fields while that on the left is almost nullified by the opposing shear forces. As a result, the cell on the right fills the cavity more than the one on the left. As Richardson number increases, the buoyancy effect is seen clearly from the evolution of streamlines in Fig. 8c for $Ri = 1$ and Fig. 8e for $Ri = 10$. For $Ri = 1.0$ in Fig. 8c and d, the cell on the right grows further with its center shifting upwards, $|\psi_{ext}| = 1.645 \times 10^{-4}$, $x = 0.76$ $y = 0.6$. For $Ri = 10$ in Fig. 8e and f, which is a buoyancy dominated regime, the counter-clockwise circulating cell on the right grows further due the aiding forces on the hot wall while the one on the left becomes weaker and smaller, i.e., the left cell nearly vanishes for the natural convection becomes more dominant there. For this case $|\psi_{ext}| = 2.44 \times 10^{-5}$, $x = 0.67$, $y = 0.51$, which shows that the center of the main cell moved towards the symmetry lines. These observations are similar to those obtained by Aydın [13] with upward moving left wall: the effect of the upward moving right wall in case III becomes negligibly small as if it were not moving. The isotherms in Fig. 8f are like observed in natural convection in differentially heated cavities and show steeper horizontal temperature gradients at the lower part of the right moving wall. Due to presence of the left cell the temperature gradient is weakened at the center of the cavity and a stratification is observed.

Velocity profiles along the centerline and local Nusselt number at the cold wall are presented in Figs. 9 and 10. Since two vertical walls move in the same direction maximum velocities are almost an order of magnitude smaller than those of the previous cases for different Richardson numbers: u velocity varies from -0.06 to 0.06 while in the other two cases it varied from -1 to 1. For cases I and II, velocity profiles are almost symmetric in lower and upper half of the cavity, which is also the case for case III except for $Ri = 0.01$. It is seen that in the latter case the profile is not symmetric, which is explained by examining the streamlines and isotherms for this case. It was seen that two quasi-symmetrical counter

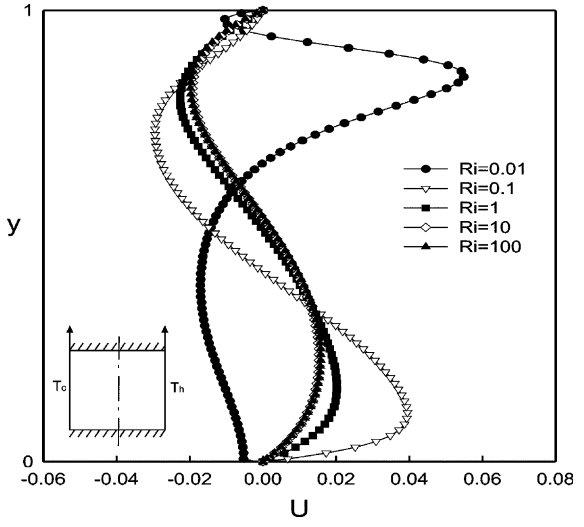

Fig. 9. Velocity profiles at the vertical centerline for case III.

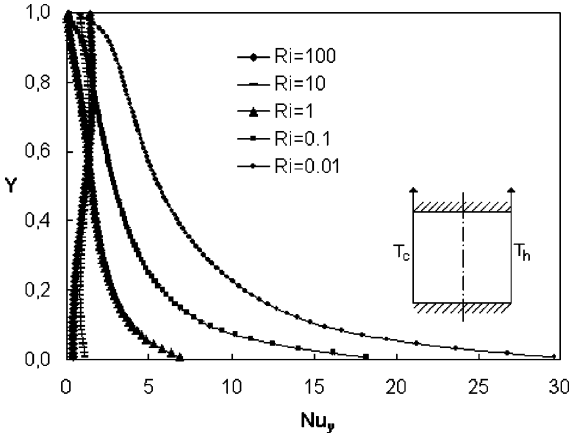

Fig. 10. Local Nusselt number along the cold wall for case III.

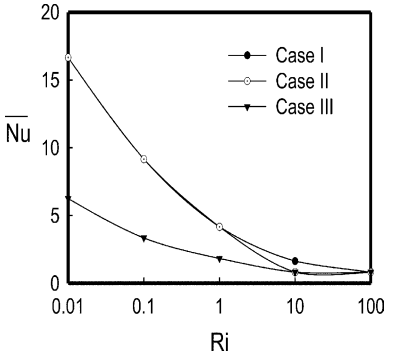

Fig. 11. Average Nusselt number for different cases as a function of Richardson number.

rotating cells were formed: the cell on the right had $|\psi_{ext}| = 1.36 \times 10^{-3}$, $x = 0.75$, $y = 0.53$ and the one on the left $|\psi_{ext}| = 1.33 \times 10^{-3}$, $x = 0.24$, $y = 0.51$. The upper part of the left cell penetrated slightly to the right hand side while the lower part of the right cell to the left hand side, resulting in the profile at the centerline shown in Fig. 9.

Fig. 10 shows that local Nusselt number is decreasing from bottom to top along the cold wall for a given Richardson number and is a decreasing function of Richardson number. It has a similar trend to that of Fig. 4, with reduced local Nusselt number. The reason is obviously due to forced convection affecting negatively the heat transfer at the cold wall.

It is noted that by changing the direction of moving sides, i.e., both downwards, we obtained exactly the same results as presented for case III.

Overall heat transfer: Finally, the average Nusselt number for three cases and different Richardson numbers are calculated using Eq. (8) and presented in Fig. 11. We should note that $Ri < 1$ is the forced convection dominated regime, $Ri > 1$ is the natural convection dominated regime and $Ri = 1$ is the mixed one. We can see that for Richardson number, $Ri < 1$, average Nusselt number variation as a function of Richardson number for cases I and II is identical and that for case III shows a similar trend but with lower values. For Richardson number, $Ri > 1$, average Nusselt number for case I is higher than that of case II and it is almost the same for cases II and III. We can also see that if the direction of the two moving walls is the same, the heat transfer is reduced and if they are moving in the opposite direction, it is enhanced. For $Ri < 1$, the heat transfer enhancement may be about three times. However, for natural convection dominated regime, i.e., $Ri > 1$, the average Nusselt number is small and has the same order of magnitude for all three cases considered, although it is slightly higher for case I. The reason for a higher heat transfer for case I is seen when we compare the strength of circulation in Figs. 2e, 5e and 8e. The same is also the case for $Ri = 100$ in Fig. 11. To understand the reason for better heat transfer for case I, we examined also streamlines and isotherms for $Ri = 100$ for all three cases: isotherms showed steeper gradients for case I compared to the other two and the strength of circulation was also stronger for that case.

6. Conclusions

This study has been concerned with the numerical modeling of mixed convection in two-sided lid-driven differentially heated cavities. It has been performed for three different cases characterized by the direction of movement of vertical walls. The governing parameter is Richardson number, which characterizes the heat transfer regime in mixed convection.

In view of the results, following findings may be summarized.

(1) The governing parameter affecting heat transfer is Richardson number $Ri = Gr/Re^2$. For $Ri < 1$, the flow and heat transfer is dominated by forced convection, for $Ri > 1$, it is dominated by natural convection and for $Ri = 1$, it is a mixed regime.
(2) For $Ri > 1$, the average Nusselt number relatively low and has the same order of magnitude for all three cases, although the heat transfer is enhanced for the case of opposing buoyancy and shear forces and for $Ri = 10$. For $Ri < 1$, the forced convection becomes dominant, the natural convection relatively weak, as a result of which Nusselt number is relatively higher.
(3) In the case of $Ri < 1$, which is the forced convection dominated regime, when the vertical walls move in opposite direction, cases I and II, the heat transfer

is considerably enhanced regardless of which side moves upwards.

(4) When the vertical walls move upwards in the same direction, case III, the heat transfer becomes reduced compared to the other two cases. This is especially discernable for $Ri < 1.0$.

(5) In case III, the lid opposing buoyancy forces decreases the heat transfer significantly by reducing the strength of the circulation regardless of which direction they move, i.e. both upwards or both downwards.

Acknowledgements

Financial support by TUBI TAK-NATO for the stay at Ecole Polytechnique is acknowledged.

References

[1] K. Torrance, R. Davis, K. Eike, D. Gill, D. Gutman, A. Hsui, S. Lyons, H. Zien, Cavity flows driven by buoyancy and shear, J. Fluid Mech. 51 (1972) 221–231.

[2] R. Iwatsu, J.M. Hyun, K. Kuwahara, Mixed convection in a driven cavity with a stable vertical temperature gradient, Int. J. Heat Mass Transfer 36 (1993) 1601–1608.

[3] N. Ramanan, G.M. Homsy, Linear stability of lid-driven cavity flow, Phys. Fluids 6 (1994) 2690–2701.

[4] R. Iwatsu, J.M. Hyun, K. Kuwahara, Convection in a differentially-heated square cavity with a torsionally-oscillating lid, Int. J. Heat Mass Transfer 35 (1992) 1069–1076.

[5] R. Iwatsu, J.M. Hyun, K. Kuwahara, Numerical simulation of flows driven by a torsionally oscillating lid in a square cavity, J. Fluids Eng. 114 (1992) 143–149.

[6] C.F. Freitas, R.L. Street, Non-linear transient phenomena in a complex recirculating flow: a numerical investigation, Int. J. Numer. Meth. Fluids 8 (1988) 769–802.

[7] R. Iwatsu, J.M. Hyun, Three-dimensional driven-cavity flows with a vertical temperature gradient, Int. J. Heat Mass Transfer 38 (1995) 3319–3328.

[8] A.A. Mohamad, R. Viskanta, Transient low Prandtl number fluid convection in a lid-driven cavity, Numer. Heat Transfer A 19 (2) (1991) 187–205.

[9] A.K. Prasad, J.R. Koseff, Combined forced and natural convection heat transfer in a deep lid-driven cavity flow, Int. J. Heat Fluid Flow 17 (5) (1996) 460–467.

[10] A.A. Mohamad, R. Viskanta, Flow and heat transfer in a lid-driven cavity with stably stratified fluid, Appl. Math. Model. 19 (8) (1995) 465–472.

[11] C.-J. Chen, H. Nassari-Neshat, K.-S. Ho, Finite-analytical numerical solution of heat transfer in two-dimensional cavity flow, Numer. Heat Transfer 4 (1981) 179–197.

[12] V.S. Arpaci, P.S. Larsen, Convection Heat Transfer, Prentice-Hall, 1984, p. 90.

[13] O. Aydın, Aiding and opposing mechanisms of mixed convection in a shear-and buoyancy-driven cavity, Int. Comm. Heat Mass Transfer 26 (1999) 1019–1028.

[14] H.C. Kuhlmann, M. Wanschura, H.J. Rath, Flow in two-sided lid-driven cavities: non-uniqueness, instabilities, and cellular structures, J. Fluid Mech. 336 (1997) 267–299.

[15] C.H. Blohm, H.C. Kuhlmann, The two-sided lid-driven cavity: experiments on stationary and time-dependent flows, J. Fluid Mech. 450 (2002) 67–95.

[16] N. Alleborn, H. Raszillier, F. Durst, Lid-driven cavity with heat and mass transport, Int. J. Heat Mass Transfer 42 (1999) 833–853.

[17] S. Acharya, F.H. Moukalled, Improvements to incompressible flow calculation on a nonstaggered curvilinear grid, Numer. Heat Transfer, Part B 15 (1989) 131–152.

[18] S.V. Patankar, Numerical Heat Transfer and Fluid Flow, Hemisphere, New York, 1980.